Biogeosciences Discuss., 12, 7055–7091, 2015
www.biogeosciences-discuss.net/12/7055/2015/
doi:10.5194/bgd-12-7055-2015

Biogeosciences Discussions
Open Access

Impacts of climate and reclamation on temporal variations in CH_4 emissions from different wetlands in China: from 1950 to 2010

T. Li[1], W. Zhang[1], Q. Zhang[1], Y. Lu[2], G. Wang[1], Z. Niu[3], M. Raivonen[4], and T. Vesala[4,5]

[1]LAPC, Institute of Atmospheric Physics, Chinese Academy of Sciences, Beijing, 100029, China
[2]Anhui Climate Center, Hefei, 230031, China
[3]State Key Laboratory of Remote Sensing Science, Jointly Sponsored by Institute of Remote Sensing Applications, Chinese Academy of Sciences and Beijing Normal University, Beijing 100101, China
[4]Department of Physics, P.O. Box 48, 00014 University of Helsinki, Finland
[5]Department of Forest Sciences, P.O. Box 27, 00014 University of Helsinki, Finland

Received: 11 April 2015 – Accepted: 23 April 2015 – Published: 12 May 2015

Correspondence to: W. Zhang (zhw@mail.iap.ac.cn)

Published by Copernicus Publications on behalf of the European Geosciences Union.

Abstract

Natural wetlands are among the most important sources of methane; thus, these areas are important for better understanding long-term temporal variations in atmospheric methane concentration. During the last 60 years, wetlands have experienced extensive conversion and global impacts from climate warming, which makes the estimation of methane emission from wetlands highly uncertain. In this paper, we present a modeling framework, integrating $CH4MOD_{wetland}$, TOPMODEL and TEM models, to analyze the temporal and spatial variations in CH_4 emissions from natural wetlands (including inland wetlands, coastal wetlands, lakes and rivers) in China. Our analysis revealed an increase of 25.5 %, averaging 0.52 g m^{-2} per decade, in national CH_4 fluxes from 1950 to 2010, which was mainly induced by climate warming. Higher rates of increasing CH_4 fluxes occurred in northeastern, northern and northwestern China, associated with large temperature increases. However, decreases in precipitation due to climate warming offset the increase in CH_4 fluxes in these regions. The CH_4 fluxes from the wetland on the Qinghai Tibetan Plateau exhibited a lower rate of increase, which was approximately 25 % of that simulated in northeastern China. Although climate warming has accelerated CH_4 fluxes, the total amount of national CH_4 emissions decreased by approximately 2.35 Tg (1.91–2.81 Tg), i.e., from 4.50 Tg in the early 1950s to 2.15 Tg in the late 2000s, due to a large wetland loss of 17.0 million ha. Of this reduction, 0.26 Tg (0.24–0.28 Tg) was derived from lakes and rivers, 0.16 Tg (0.13–0.20 Tg) from coastal wetlands, and 1.92 Tg (1.54–2.33 Tg) from inland wetlands. Northeastern China had the largest contribution to this reduction, with a loss of 1.68 Tg. The CH_4 emissions were reduced by more than half in most regions in China except for the Qinghai Tibetan Plateau, where only a 23.3 % decrease in CH_4 was observed.

1 Introduction

Atmospheric methane (CH_4) is the second most important trace greenhouse gas (GHG) after carbon dioxide (CO_2). The direct radiative forcing for CH_4 is 25 times greater than that of CO_2 over a 100 year period (IPCC, 2007). In the atmosphere, the direct radiative forcing of CH_4 was calculated to be 0.48 $W m^{-2}$ by IPCC (2007); this value was revised to 0.97 $W m^{-2}$ when its indirect global warming effect was incorporated (IPCC, 2013; Forster et al., 2007; Shindell et al., 2009). In 2011, the concentration of atmospheric CH_4 reached 1803.2 ppb, which was 150 % greater than before 1750 (IPCC, 2013). However, unlike the rigid temporal increase of atmospheric CO_2, atmospheric CH_4 has exhibited remarkable temporal variations in conjunction with a long-term increasing trend, e.g., remaining nearly constant from 1999 to 2006, then continuing to increase after 2007 (Nisbet et al., 2014).

While the majority of CH_4 sinks remain relatively stable, variations in atmospheric CH_4 have been attributed to these sources. Among the global CH_4 emission sources, natural wetlands are one of the most important contributors (Denman et al., 2007; Potter et al., 2006; Whalen, 2005). The methane emissions from wetlands account for 20–25 % of the global annual atmospheric emissions, although the uncertainties are relatively large (IPCC, 2007; Mitsch and Gosselink, 2007). During the 20th century, half of the world's wetlands were lost (Moser et al., 1996; Revenga et al., 2000). In China, natural wetlands have also experienced a serious loss during the past 60 years, attributed primarily to cropland reclamation (An et al., 2007; Niu et al., 2012; Huang et al., 2010; Xu and Tian, 2012). Based on remote sensing data, Niu et al. (2012) reported that approximately 33 % of the wetlands were lost between 1978 and 2008. An et al. (2007) estimated that 23 % of freshwater swamps, 16 % of lakes, 15 % of rivers, and 51 % of coastal wetlands were lost between 1950 and 2000 based on census data.

Multiple studies for estimating CH_4 emissions in China have been conducted; most of these works have involved the extrapolation of site-specific measurements to the region (Wang et al., 1993; Khail et al., 1993; Jin et al., 1999; Ding et al., 2004, 2007; Chen

BGD
12, 7055–7091, 2015

et al., 2013; Wang et al., 2012). However, substantial spatial and seasonal variations in CH_4 emissions from natural wetlands are often observed (e.g., Christensen et al., 2003; Ding et al., 2004; Yang et al., 2006) because of the complex physiological processes of plants and microorganisms, which are regulated by climatic and edaphic factors (Cao et al., 1998).

Some modelers have simulated national CH_4 emissions from marshlands for the last 60 years (e.g., Xu and Tian, 2012; Tian et al., 2011) based on census data collected in areas that were historically wetlands. To date, there has been no comprehensive study on national, long-term CH_4 emissions from all natural wetlands, including freshwater marshes, coastal wetlands, lakes and rivers in China.

A remote sensing study presented a comprehensive map of the change in natural wetlands that occurred between 1978 and 2008 in China (Niu et al., 2012). The objectives of the present study are to analyze the spatial and temporal changes in CH_4 emissions across China's natural wetlands to quantify the impact of climate change and anthropogenic activities on CH_4 emissions from the natural wetlands in different regions of China.

2 Materials and methods

In this research, the primary natural wetland types include coastal wetlands, lakes and rivers, and other types that are defined as inland wetlands (e.g., marshes, peatlands, and floodplains). In the present study, we used a modified biogeophysical model, called $CH4MOD_{wetland}$ (Li et al., 2010), to simulate CH_4 emissions from inland wetlands and coastal wetlands. Because $CH4MOD_{wetland}$ is not capable of simulating CH_4 emissions from lakes and rivers, we directly extrapolated site-level field measurements (see Supplement S1) to estimate the CH_4 emissions from lakes and rivers (Chen et al., 2013).

2.1 Model framework

Figure 1 shows the model framework for this study. Three models were used with a spatial resolution of 0.5° for the period from 1950 to 2010. The main model was a process-based biogeophysical model, i.e., $CH4MOD_{wetland}$ (Li et al., 2010). This model simulated CH_4 fluxes and with inputs of soil texture (soil sand fraction, soil organic carbon and bulk density), wetland area, aboveground net primary productivity (ANPP), daily soil temperature, water table depth and salinity. To make the model useful for coastal wetlands, some modifications were made. For details concerning the modifications made to $CH4MOD_{wetland}$, please see Supplement S2.

To obtain regional datasets of ANPP, soil temperature and water table depth for use at a national scale, we used the outputs of the Terrestrial Ecosystem Model (TEM) (Melillo et al., 1993; Zhuang et al., 2004, 2006; 2007, 2013) and the TOPMODEL (Beven and Kirby, 1979) to drive $CH4MOD_{wetland}$.

The TEM model is also a process-based biogeochemistry model that couples carbon, nitrogen, water, and heat processes in terrestrial ecosystems to simulate ecosystem carbon and nitrogen dynamics. This model has been widely used to investigate regional and global NPP (e.g., Melillo et al., 1993; Cramer et al., 1999; McGuire et al., 1992). With this model framework (Fig. 1), the soil temperature and net primary productivity (NPP) outputs from the TEM model were used to drive $CH4MOD_{wetland}$. The fraction of ANPP to NPP was determined based on Gill and Jackson (2003). More descriptions of the model and the inputs are described in Zhuang et al. (2013).

TOPMODEL is a conceptual rainfall–runoff model that is designed to work at the scale of large watersheds using the statistics of topography. In previous research (Bohn et al., 2007; Kleinen et al., 2012; Lu and Zhuang et al., 2012; Zhu et al., 2013), TOPMODEL has been widely used to simulate water table variations in natural wetlands. The TOPMODEL inputs included soil moisture and the topographic wetness index (Fig. 1). The outputs (water table depth) were used to drive $CH4MOD_{wetland}$ (Fig. 1).

More details on simulating water table depth using TOPMODL are provided in Supplement S2.

2.2 Model calibration

In previous studies, we parameterized the model using independent CH_4 flux measurements collected from the Sanjiang Plain (SJ site in Table S2) (Li et al., 2010, 2012). We also validated the model at wetland sites in the United States and Canada, with most parameters remaining unchanged (Li et al., 2010). In the present study, two parameters associated with plant species, i.e., the vegetation index (VI) and the fraction of CH_4 oxidized during plant mediated transport (P_{ox}), were recalibrated for a wetland site dominated by *Phragmites* (Table S2). We parameterized VI and P_{ox} by minimizing the differences between the observed and simulated fluxes at Wuliangsu Lake in Inner Mongolia (WLS site in Table S2). By setting an increment of 0.1 for VI and P_{ox}, the model was run for all combinations of VI within the range 0.5–3.0 and P_{ox} within the range 0.1–1 until the root-mean-square error (RMSE) between the daily simulated and observed CH_4 fluxes was minimized. After setting VI and P_{ox}, the empirical constant of the salinity influence *a* (Eq. (S2.1) in Supplement S2) was calibrated (attaining a value of −0.025) by minimizing the root mean-square error (RMSE) between the observed and simulated fluxes at a coastal wetland on Chongming Island in Shanghai Province (CMI site in Table S2). Table S3 shows the value of the main parameters and inputs used for simulating the CH_4 emissions at the different sites.

2.3 Model validation

After model coupling and calibration, model validation is necessary to determine if the model can be used at a national scale. We used independently observed data (different than the data that was used to calibrate the model) to validate the model at the "site-scale" using individual $CH4MOD_{wetland}$ simulations and at the "grid-scale" using the

BGD
12, 7055–7091, 2015

proposed model framework (Fig. 1). More details regarding the "site-scale" and the "grid-scale" validations are described in Supplement S2.

The "site-scale" validation showed that the simulated seasonal patterns of daily CH_4 emissions agreed with the observed data at the wetland sites on the Sanjiang Plain (Fig. S1a and b), the Ruoergai Plateau, (REG in Table S2; Fig. S1d and e), the Haibei alpine marsh (HB in Table S2; Fig. S1g), the Zhalong wetland (ZL in Table S2; Fig. S1i) and the Liao River delta (LRD in Table S2; Fig. S1k). The regression of simulated vs. observed monthly CH_4 fluxes resulted in an R^2 of 0.79, with a slope of 0.86 and an intercept of 0.73 ($n = 41$, $p < 0.001$) for the "site-scale" validation (Fig. S2a). The RMSE, mean deviation (RMD) and the model efficiency (EF) between the simulated and observed monthly CH_4 fluxes were 48.5, 0.9 % and 0.78, respectively.

The "grid-scale" validation showed that the integrated model framework ($CH4MOD_{wetland}$/TEM/TOPMODEL) (Fig. 1) was able to simulate the seasonal variations in monthly CH_4 emissions at the SJ (Fig. S1c) and LRD (Fig. S1l) sites. Although there are some underestimations in the CH_4 fluxes were predicted by the model framework for the other 3 sites (Fig. S1f, h and j), the measured monthly CH_4 fluxes fell in or near the range of the modeled CH_4 emissions (Fig. S2b). For the "grid-scale" validation, the regression of simulated vs. observed monthly CH_4 emissions resulted in an R^2 of 0.79, with a slope of 0.84 and an intercept of −0.11 ($n = 41$, $p < 0.001$). The RMSE, RMD and EF between the simulated and observed monthly CH_4 fluxes were 51.3, −17.8 % and 0.75, respectively, for the integrated model framework.

2.4 The extrapolation of the model framework

The extrapolation of this model framework to the national scale (Fig. 1) was based on a wetland division map (Lang and Zu, 1983) (Fig. 2) and a gridded wetland distribution map (Niu et al., 2012) (Fig. 2) of China. Chinese wetlands were divided into five regions according to the location and vegetation type. More details regarding the division of the wetlands are described in Supplement S3. For the inland wetlands, we classified the parameters according to the wetland division map. We extrapolated the parameters

BGD
12, 7055–7091, 2015

from a wetland site to the region in which it is located. The model parameters at SJ, HB, and WLS (Table S3) were assigned to Region I, Region II and Region III, respectively. In Region IV, we used the parameters for WLS because *Phragmites* is the dominant species in both Region III and Region IV (Table S2). The model parameters for REG (Table S3) were allocated to Region V because this wetland is located at the edge of this region. The coastal wetland parameters were assigned to LRD and CMI (Table S3).

The gridded wetland distribution maps were presented by Niu et al. (2012) at a resolution of 1 km × 1 km. We compiled the data from the gridded wetland maps to generate a dataset of 0.5° × 0.5° spatial resolution. We established gridded (0.5° × 0.5°), georeferenced, time-series input datasets of climatic factors (including daily temperature, precipitation, humidity, and solar radiation) and the soil data (including soil sand percentage, soil bulk density, soil organic carbon and the soil moisture), the water table data and the salinity data for all of China. The climate and soil texture data were used to drive the TEM model (Fig. 1). The soil moisture and topographic wetness index data were used as inputs for TOPMODEL (Fig. 1). Then, $CH4MOD_{wetland}$ was run with the ANPP, soil temperature, water table depth, soil texture, and salinity data in each grid cell to estimate the CH_4 fluxes (Fig. 1). The total CH_4 emissions from each grid cell were determined based on the product of the CH_4 fluxes and the wetland area.

2.5 Uncertainty analysis

Uncertainty in the estimated regional CH_4 emissions from natural wetlands may originate from many factors. In this study, we paid more attention to the uncertainties induced by the inputs of ANPP, water table depth and soil sand fraction using the extreme condition approach for uncertainty propagation (Du and Chen, 1999; Li et al., 2012). We set the maximum and minimum values of the input data to be ±10 % of the baseline values. Eight simulations were performed to estimate the uncertainties.

BGD
12, 7055–7091, 2015

2.6 Data sources

We selected seven natural wetlands where extensive field measurements were available for model calibration and model validation. These sites included two marshes, two floodplains, one peatland and two coastal wetlands (Table S2). Figure 2 shows the locations of the sites. More detailed site descriptions are provided in Table S2.

The gridded wetland maps for 1978, 1990, 2000 and 2008 were obtained from Niu et al. (2012). The method for obtaining the gridded wetland map for 1950 was based on both Niu et al. (2012) and An et al. (2007). An et al. (2007) reported that inland wetland areas lost 23.0 %, lake areas lost 16.1 %, river areas lost 15.3 %, and coastal wetland areas lost 51.2 % of their area between 1950 and 2000 in China. To use inland wetlands as an example, we first separated the Sanjiang Plain because more detailed and accurate data could be obtained for that area. Then, we assumed the annual loss rate of inland wetlands was constant between 1950 and 2000. We calculated the annual loss of the inland wetlands between 1950 and 2000 based on An et al. (2007). We regarded this ratio as the annual loss rate of inland wetlands between 1950 and 1978. We also assumed this annual loss rate occurred in every inland wetland grid cell. The inland wetland area in each grid cell in 1950 was determined using the above annual loss rate as well as the wetland area reported to exist in 1978 based on Niu et al. (2012). Niu et al. (2012) combined floodplains and rivers as river wetlands in his paper; however, because floodplains are always dominated by vascular plants, we included floodplains in the inland wetland category. The fraction of floodplains was based on original satellite data (Z. G. Niu, personnal communication, 2013). The wetland area included from the Sanjiang Plain in 1950 was from previous studies (Liu and Ma, 2000; Li et al., 2012; Huang et al., 2010; Ding et al., 2004, 2007). The method used to calculate the lake, river and coastal wetland areas was the same as for the inland wetlands.

Daily climate datasets used for driving the TEM model were developed from the latest monthly air temperature, precipitation, vapor pressure, and cloudiness datasets

BGD
12, 7055–7091, 2015

from the Climatic Research Unit (CRU TS 3.10) of the University of East Anglia in the United Kingdom (Harris et al., 2014).

The soil moisture data were from Fan and van den Dool (2004) (http://www.cpc.ncep.noaa.gov/soilmst/leaky_glb.htm). The soil texture data were derived from the soil map of the Food and Agriculture Organization (FAO, 2012). Soil sand fraction data were used as input to $CH4MOD_{wetland}$, whereas, soil texture data were used to assign the texture-specific parameters to each grid cell in the TEM model (Zhuang et al., 2013). Soil organic carbon content and the reference bulk density in wetland soils were from the Harmonized World Soil Database (HWSD) (FAO, 2008).

The vegetation map of IGBP was referenced to specify vegetation parameters for $CH4MOD_{wetland}$ and TEM. The map was derived from the IGBP Data and Information System (DIS) DISCover Database (Belward et al., 1999; Loveland et al., 2000). The 1 km × 1 km DISCover dataset was reclassified into the TEM vegetation classification scheme and then aggregated to a resolution of 0.5° × 0.5°.

The topographic wetness index data were from the HYDRO1k Elevation Derivative Database, which was developed by the U.S. Geological Survey Earth Resources Observation and Science (EROS) Center (http://gcmd.nasa.gov/records/GCMD_HYDRO1k.html) (USGS, 2000). The global salinity database was from the World Ocean Atlas 2009 (Antonov et al., 2010).

3 Results

3.1 CH_4 fluxes with changes in climate from 1950 to 2010

The temporal change in CH_4 fluxes (CH_4 emissions per area) were determined based on the climate. In this section, we analyze the climate change-driven interannual variations in CH_4 fluxes from the inland wetlands and the coastal wetlands from 1950 to 2010. Figure 3f provides the interannual variation and trend in the modeled national annual CH_4 flux in China. The national annual CH_4 flux significantly increased over

BGD
12, 7055–7091, 2015

the last 60 years, especially since the 1980s. The national annual CH_4 flux increased from 16.9 $g\,m^{-2}\,yr^{-1}$ in 1950 to 21.2 $g\,m^{-2}\,yr^{-1}$ in 2010, a total increase of 26 % or an average rate of 0.52 $g\,m^{-2}$ per decade. The annual CH_4 fluxes fluctuated between 16.0 and 19.0 $g\,m^{-2}\,yr^{-1}$ before 1980, then increasing rapidly in the 1990s. The highest CH_4 flux, i.e., 22.5 $g\,m^{-2}\,yr^{-1}$, occurred in 1998, whereas the lowest value, 15.7 $g\,m^{-2}\,yr^{-1}$, occurred in 1954.

The estimated annual CH_4 fluxes in different regions are illustrated in Fig. 3a–e. The regions with the largest CH_4 fluxes are northeastern China (Region I, with an average annual mean of 24.8 $g\,m^{-2}\,yr^{-1}$; Fig. 3a) and southern China (Region V, with an average annual mean of 20.1 $g\,m^{-2}\,yr^{-1}$; Fig. 3e). On the Qinghai Tibetan Plateau (Region II), the simulated CH_4 fluxes exhibited the lowest fluxes (Fig. 3b), with an average annual mean of 6.2 $g\,m^{-2}$ over the same period, which was lower than Region I by approximately 75 % (Fig. 3a). Compared with Region I, the average CH_4 fluxes in Inner Mongolia and northwestern China (Region III) and over the North China Plain and the Middle-Lower Yangtze Plain (Region IV) were lower by 46 to 64 % during the past 60 years.

Figure 3 also provides the trends in the annual CH_4 fluxes in different regions. Except for Region IV (Fig. 3d; $p > 0.05$), the annual CH_4 fluxes exhibited significant increases in other regions (Fig. 3a–e; $p < 0.001$). The greatest rate of increase in CH_4 fluxes occurred in Region I, i.e., 0.67 $g\,m^{-2}$ per decade (Fig. 3a), followed by Region V and Region III, i.e., 0.54 $g\,m^{-2}$ per decade (Fig. 3e) and 0.42 $g\,m^{-2}$ per decade (Fig. 3c), respectively. In Region IV, the rate of increase in CH_4 fluxes was 0.50 $g\,m^{-2}$ per decade, although this rate was not significant (Fig. 3d). The smallest rate of increase occurred in Region II (Fig. 3b), i.e., approximately 25 % of the rate for Region I (Fig. 3a).

Climate factors can account for the difference in the rates of increase in CH_4 fluxes among the regions noted above. First, a higher temperature will enhance the rate of microbial CH_4 production. Second, an increase in precipitation may result in a higher water table position and promote plant growth, which can accelerate CH_4 fluxes. We

BGD
12, 7055–7091, 2015

analyzed the effects of air temperature (T_{air}) and precipitation (P) based on the five-year average CH_4 fluxes in each region (Fig. 4).

The modeled five-year CH_4 fluxes exhibited linear trends that closely follow the trends in air temperature in Region I (Fig. 4a), Region II (Fig. 4b), Region III (Fig. 4c) and Region V (Fig. 4e), suggesting that during the past 60 years, the increased CH_4 fluxes were primarily by climate warming. The contribution of precipitation to the trends in CH_4 fluxes differed among the regions. During the past 60 years, Region I and Region III experienced large temperature increases (rates of 0.29 °C per decade and 0.34 °C per decade, respectively). These increases resulted in higher rates of increase in CH_4 fluxes, i.e., 0.67 g m^{-2} per decade (Fig. 3a) and 0.42 g m^{-2} per decade, respectively (Fig. 3c). In Region I, CH_4 fluxes were predominantly positively correlated with air temperature ($R^2 = 0.35$, $p < 0.001$) (Fig. 4a). Although no correlation was found between the CH_4 fluxes and the precipitation in Region I, the linear precipitation decrease of 38.3 mm per decade ($p < 0.001$) may have offset the increase in CH_4 fluxes due to the air temperature (Fig. 4a) before 1980. The linear precipitation decrease of 1.7 mm per decade ($p = 0.4$, not significant) in Region III may also have a negative impact on CH_4 fluxes (Fig. 4c). CH_4 fluxes in Region II showed a positive correlation with both temperature and precipitation (Fig. 4b). A slight temperature increase of 0.19 °C per decade and precipitation increase of 6.7 mm per decade resulted in a flux increase of 0.17 g m^{-2} per decade. In Region V, the positive correlation between CH_4 fluxes and temperature was more significant than with that of precipitation (Fig. 4e), suggesting that the temperature was the dominant factor in the acceleration of CH_4 fluxes during the past 60 years. The increase in the precipitation, at a rate of 16.6 mm per decade, although not significant ($p = 0.24$), may have benefited the CH_4 fluxes in this region. In Region IV, CH_4 fluxes were less responsive to temperature than precipitation (Fig. 4d). The increase in temperature still promoted CH_4 fluxes to increase at a rate of 0.50 g m^{-2} per decade, although this rate was not significantly (Fig. 3d).

Interannual or interdecadal variations in CH_4 fluxes were found to be closely aligned with variations in precipitation (Fig. 4). The lowest CH_4 fluxes usually accompanied

BGD
12, 7055–7091, 2015

periods with low precipitation. For example, the lowest CH_4 fluxes and precipitation occurred simultaneously during the period 1980–1985 in Region IV (Fig. 4d) and the period 1965–1970 in Region V (Fig. 4e). In Region I, the five-year average CH_4 fluxes showed a trend that was synchronous with the five-year average precipitation trend (Fig. 4a), first decreasing before 1980 and then increasing until 1995. In Region I and Region II, excessive amounts of precipitation fell in the 1990s (Fig. 4a) and 2000s (Fig. 4b) in conjunction with relatively high air temperatures, which resulted in the highest CH_4 fluxes found in this study. In contrast, when the greatest amount of precipitation occurred (Fig. 4c: from 1955 to 1960 in Region III, Fig. 4d: from 1960 to 1975 in Region IV, and Fig. 4e: from 1970 to 1975 in Region V), the CH_4 fluxes remained low due to the lower air temperatures.

3.2 Changes in regional CH_4 emissions resulting from climate change and wetland loss

The total wetland area in China was approximately 35.6 million ha in 1950 (Table 1). Wetland loss was 17.0 million ha from 1950 to 2010, nearly half of the existing wetland area in 1950. During the first 50 years, wetland areas decreased by 16.1 million ha. Since 2000, wetland loss has been more limited (Table 1).

A tremendous wetland loss occurred in Region I, 7.8 million ha, accounting for approximately 45.7 % of the total wetland loss (Table 1). Compared with 1950, the wetland areas decreased by 56.9, 24.6, 48.4, 65.3 and 46.7 % in Region I, Region II, Region III, Region IV and Region V (Table 1), respectively.

Among the wetland types, the greatest loss occurred in inland wetlands, with a total loss of 10.3 million ha from 1950 to 2010, accounting for 60.6 % of the total wetland loss. More than 95 % of the inland wetland loss occurred in Region I, Region II and Region III (Table 1). In contrast, coastal wetland loss occurred primarily in eastern and southern China (Region IV and Region V) (Table 1). The coastal wetland losses were 68.5 % in 2008 compared to their area in 1950. The total area loss was 4.94 million ha for lake and river wetlands between 1950 and 2008. Substantial loss of lakes/rivers occurred in eastern China (Region IV).

CH_4 emissions decreased by approximately 2.35 Tg (1.91–2.81 Tg) in China's wetlands, i.e., from 4.50 Tg in the early 1950s to 2.15 Tg in the late 2000s (Table 1). More than 99 % of the CH_4 reduction occurred before 2000, which was in accordance with the wetland loss trend (Table 1).

On a national scale, the wetlands in Region I were the greatest source of the decreased CH_4 fluxes, corresponding to areas with significant wetland losses (Table 1) and the highest CH_4 fluxes (Fig. 2b). In Region I, CH_4 emissions decreased by 58.3 % in the late 2000s compared with the early 1950s, with a loss of 1.68 Tg (1.36–2.03 Tg) (Table 1). In other regions, the reduction in CH_4 emissions was 0.13–0.19 Tg, with a loss fraction of 23.3–57.6 % (Table 1). Among the regions, the lowest CH_4 reduction occurred in Region II, where only a slight loss in wetlands occurred. The loss fraction of CH_4 emissions was 23.3 %, which is comparable to the wetland loss area (i.e., 24.6 %) between 1950 and 2008 in this region (Table 1).

Methane emissions decreased by 54.4, 62.9 and 37.1 % in inland wetlands, coastal wetlands and lakes/rivers, respectively (Table 1). Region I was the most important contributor to the decreased CH_4 emissions, which contributed 85.4 % to the regional CH_4 reduction for inland wetlands (Table 1). For the coastal wetlands, substantial CH_4 reduction occurred in Region V. The CH_4 fluxes decreased by nearly 82.4 % from the early 1950s to the late 2000s in the coastal wetlands of this region (Table 1). Although the coastal wetland loss was higher in Region IV than in Region V, the CH_4 reduction in Region IV was only 21 % of that in Region V (Table 1). This difference was because the CH_4 fluxes in the coastal wetland were 2.4 times greater in Region V than in Region IV (compare Fig. 3e with Fig. 3d).

BGD
12, 7055–7091, 2015

Title Page
Abstract Introduction
Conclusions References
Tables Figures
Back Close
Full Screen / Esc
Printer-friendly Version
Interactive Discussion

4 Discussion

4.1 Plant growth and impacts on CH_4 emissions

Plants can enhance CH_4 production by providing methanogenic substrates and by functioning as conduits for CH_4 transport through the aerenchyma system. Conversely, plants can attenuate CH_4 emission by facilitating CH_4 oxidation through the transport and release of O_2 from roots located in anoxic peat (Whalen, 2005; Ding et al., 2005). Previous studies on pulse-labeling experiments reported a 1–3 % recovery of photo-assimilated C as $^{14}CH_4$ in observational periods of 2 to 10 weeks (Wieder and Yavitt, 1994; Loya et al., 2002; King et al., 2002; King and Reeburgh, 2002). For example, King et al. (2002) estimated that more than 75 % of the average CH_4 emissions from tundra wetlands originated from recently fixed carbon. However, other studies (Megonigal et al., 1996; Juutinen et al., 2003; Ding et al., 2002) have found that recent photosynthates of wetland plants provide a very limited contribution to CH_4 production, and labile organic C for CH_4 production is mainly derived from plant litter.

Many studies have indicated that most CH_4 emitted from the wetlands is mediated by aerenchymatous plants (Cicerone and Shetter, 1981; Holzapfel-Pschorn et al., 1986; Chanton et al., 1989; Waddington and Roulet, 1996). However, the ventilative and diffusive activities that transport CH_4 to the atmosphere also oxygenate the rhizosphere, creating favorable conditions for CH_4 oxidation in this otherwise anoxic, CH_4-rich zone (King, 1994; Calhoun and King, 1997, 1998). The ability of aerenchymatous plants to act as a transporter differs among species (Whalen, 2005). The different transport controls may be related to plant architecture (Schimel, 1995).

The current knowledge of the effects of plants on CH_4 production and emission are insufficient and difficult to quantify for various plants. In $\text{CH4MOD}_{\text{wetland}}$, the plant-related parameters include the vegetation index (VI), the fraction of plant-mediated transport (T_{veg}), and the fraction of CH_4 oxidized during plant-mediated transport (P_{ox}) (Table S3). We calibrated the above parameters, focusing on sites with *Carex* and *Phragmites* (Tables S2 and S3), although these calibrations were not sufficient for use

BGD
12, 7055–7091, 2015

throughout the entire country. For example, mangroves are mainly species of coastal wetlands in southern China; however, we have no calibration and validation due to a lack of measurements. The plant species are abundant and diverse in Chinese wetlands (Supplement S3). More experiments are needed to accurately parameterize the different plant species so that the regional estimate will be more reliable.

4.2 Variation in water table depth with climate change

The water table depth divides the anaerobic and aerobic zone and regulates the soil redox potential (Yu et al., 2001). CH_4 fluxes are strongly controlled by the water table depth. Previous measurements have consistently demonstrated that CH_4 emissions decline following short- and long-term water table drawdown (Laiho, 2006; Turetsky et al., 2008). Short-term water table drawdown experiments have displayed decreased CH_4 emissions ranging from 17 to 150 % depending on the extent of water table drawdown and vegetation community structure (Dise et al., 1993; Aerts and Ludwig, 1997; Strack and Waddington, 2007; Turetsky et al., 2008). Long-term (> 30 year) water table drawdown studies found 67 to 96 % decreases in CH_4 emissions (Yrjala et al., 2011; Nykanen et al., 1998; Ballantyne et al., 2014). Model sensitivities also show that water table depth is one of the most sensitive factors to CH_4 emissions (Boon, 1997; Zhu et al., 2013; Li et al., 2010). Thus, without proper information regarding water table positions, estimates of CH_4 are poorly constrained (Fan and Miguez-Macho, 2011).

Much progress has been made in estimating regional CH_4 emissions. However, large uncertainties remain in estimating emissions due to the spatial variability in water table depth. The TOPMODEL-based scheme (Bevenand Kirkby, 1979) has been widely used to model regional water table depth in natural wetlands (Zhu et al., 2013; Lu and Zhuang, 2012; Kleinen et al., 2012) because it is a flexible mass balance modeling tool that can be linked to biogeochemical models. TOPMODL is based on the topographic wetness index (TWI) and assumes that water tables follow topography holds (Haitjema and Mitchell-Bruker, 2005). However, the TWI is static and relies on the assumption that the local slope, i.e., $\tan\beta$, is an adequate proxy for the effective downslope hy-

BGD
12, 7055–7091, 2015
CH_4 from Chinese natural wetlands
T. Li et al.

draulic gradient, which is not necessarily true in low-relief terrain (Grabs et al., 2009). Therefore, this algorithm is less suitable in flat areas and will induce uncertainties in the simulated water table depth. Moreover, the precision of the TWI data is important for the accuracy of the results. The HYDRO1k global values for the TWI provided by the USGS in 2000 (USGS, 2000) are the most commonly used data for the TOPMODEL method. However, the limited resolution and quality of the data can induce uncertainties, especially in tropical wetlands (Marthews et al., 2015; Collins et al., 2011). In the future, more accurate descriptions of the hydrology process and higher-resolution datasets are needed to reduce the error in the simulated water table depth.

4.3 Regional estimates of CH_4 emissions

Estimates of CH_4 emissions from natural wetlands in China are highly uncertain, with a range of 1.7 to 10.5 Tg (Table 2). We estimated that the CH_4 emissions were 2.17–3.03 Tg during from 1990 to 2000, which falls within the reported range.

Previous studies have primarily extrapolated measurements to encompass all of China (Wang et al., 1993, 2012; Khalil et al., 1993; Jin et al., 1999; Ding et al., 2004; Chen et al., 2013; Cai, 2012) (Table 2). However, this may induce uncertainties because CH_4 fluxes exhibit substantial variation according to wetland type and within different climatic and soil environments (Cao et al., 1998). For example, the estimations of both Ding and Chen were primarily based on measurements from the Ruoergai Plateau, which is located along the eastern edge of Qinghai Tibetan Plateau (Chen et al., 2013; Ding et al., 2004). However, Chen used an observation of CH_4 fluxes that was much higher than Ding's observation, resulting in substantially higher emission estimates for the Qinghai Tibetan Plateau (Table 2).

Based on atmospheric CH_4 concentrations, Zhang et al. (2013) provided an estimation of 4.76 Tg (Table 2), which is twice the estimated CH_4 emissions presented in this study. The use of retrieved atmospheric concentrations as a method for estimating the CH_4 sources is challenging because of the sparse observation network.

BGD
12, 7055–7091, 2015

Compared with the above methods, process-based models that describe major biogeochemical behaviors influencing the processes of CH_4 production, oxidation and emission are potentially effective tools for long-term regional estimation. Previous studies (Table 2) have focused primarily on estimating CH_4 emissions after the 1990s, except for Xu and Tian (2012) (Table 2), who inferred a reduction of approximately 1.3 Tg CH_4 from Chinese marshlands between 1949 and 2008 due to marshland conversion and climate change. This study and Xu's study have similar objectives and results, although there are some differences between the two studies.

First, Xu's study only focused on marshlands (the definition of marshland in his paper is natural wetland that is not coastal wetlands, lakes and rivers), which is the same wetland type use for inland wetlands in this study. However, this study includes coastal wetlands, lakes and rivers, which represent approximately 40 % of the wetland loss (Table 1). To the best of our knowledge, this study provides the first national estimates of long-term CH_4 emissions from China's natural wetlands.

Second, in Xu's study, the marshland distribution was derived from land-use data in China (Liu et al., 2005; Liu and Tian, 2010). The annual marshland area was interpolated using a negative correlation between the Chinese population and censused marshland area between 1950 and 2000. However, this relationship inevitably resulted in large uncertainties because human activity was not the only driving factor in wetland loss (Niu et al., 2012). For example, drought induced by climate warming is the main reason for the wetland loss on the Qinghai Tibetan Plateau (Niu et al., 2012). We used the latest wetland area satellite data for the four studies periods and the census data to inversely determine the initial wetland area (see materials and methods), which was found to be more accurate and acceptable, especially after 1980. As a result, Xu estimated decreases of 8.5 million ha in the marshland area and approximately 1.3 Tg in CH_4 emissions between 1950 and 2008 (Table 2). We estimated a reduction of 10.3 million ha and 1.9 Tg during the same period (Tables 1 and 2). The most significant difference occurred after 1980 (Table 2). The CH_4 fluxes were estimated to decrease by 0.4 and 1.1 Tg in Xu's study and in this study, respectively, between the early 1980s

BGD
12, 7055–7091, 2015

and the end 2000s. This difference was because the marshlands and wetland losses considered by Xu represented only half of the wetlands and wetland losses that were considered in this study. Spatially, in southwestern China (Region II), we estimated a marshland loss of 1.6 million ha, i.e., from 4.8 to 3.2 million ha (Tables 1 and 2). In Xu's study, the marshland area decreased by 0.2 million ha, i.e., from 0.8 to 0.6 million ha, which may have underestimated the wetland loss because the estimate relied solely on the relationship between population and marshland area.

Finally, the model DLEM (Xu's model) calibration and validation were primarily based on measurements collected in marshlands dominated with *Carex*. However, some important parameters in DLEM are related to the ambient vegetation, such as the maximum rate of CH_4 oxidized through plant transportation and the half-saturation coefficient of CH_4 oxidized through plant transportation In Inner Mongolia, northwestern China, the North China plain and the Middle-Lower Yangtze Plain, *Phragmites* represent the primary vegetation type (see Supplement S3). Although *Phragmites* usually have larger biomass than *Carex*, the CH_4 fluxes are lower (according to a comparison between CH_4 fluxes in the perennial inland wetlands in WLS, ZL and SJ in Fig. S1; Table S2). If the parameters for *Carex* are used for the regions dominated by *Phragmites*, the results may be overestimated. This difference can explain why the CH_4 reduction contributed 21.2 % in northwestern and northern China (including Region III and Region IV in this study) in Xu's study. However, in this study, this contribution was found to be only 7.3 %.

There are several factors that may introduce uncertainties into regional estimates. The data sources for wetland areas may induce uncertainties, especially for the 1950s. In addition, due to the high spatial heterogeneity, uncertainties may be produced due to the limited resolution in the model upscaling. For example, there is substantially heterogeneity in the water table depth and the NPP at a resolution of 0.5°. Although we compared the simulated and observed gridded CH_4 fluxes (Figs. S1 and S2), the average input data inevitably misses the heterogeneity in the CH_4 fluxes within each

BGD
12, 7055–7091, 2015

grid cell. As a result, the "grid-scale" model performance was not as good as the site-level model performance (Figs. S1 and S2).

4.4 Future trends in CH_4 emissions from Chinese wetlands

According to China's National Assessment Report on Climate Change (Ding and Ren, 2007), compared with the period 1961–1990, there will be a pronounced air temperature increase of 3.6–4.9 °C based on the A2 and B2 scenarios (IPCC, 2000) by the end of this century in China. The precipitation is also predicted to increase by 9–11 % for the A2 and B2 scenarios by 2100. The air temperature and precipitation increases differ between individual regions (Fig. 4). Depending on the regional conditions and wetland types, the consequences of future climate change on CH_4 fluxes will be spatially different and depend on regional and wetland characteristics.

Warming is expected to promote CH_4 fluxes from wetlands in the future (Zhuang et al., 2006; Christensen and Cox, 1995; Shindell et al., 2004). The air temperature is expected increase more rapidly in northeastern China (Region I), northwestern China (Region III) and the North China Plain (the inland wetlands in Region IV) (Ding and Ren, 2007), which indicates that there will be a larger promotion of CH_4 fluxes from the inland wetlands in these regions. For the Qinghai Tibetan Plateau (Region II), eastern China (the coastal wetlands in Region IV), and southern China (Region V), the climate-induced increase in CH_4 fluxes from inland and coastal wetlands will be lower.

However, if precipitation remains unchanged, warming conditions will be accompanied by increased drought and rising sea levels (Lin et al., 2011), which will produce a negative impact on regional CH_4 emissions. For the inland wetlands, such as the marshlands of the Sanjiang Plain (Region I) and the peatlands of the Qinghai Tibetan Plateau (Region II), drought conditions will increase evapotranspiration, decrease the anti-interference ability of wetlands, speed up wetland degradation (Liu et al., 2001), and ultimately decrease CH_4 fluxes and regional CH_4 emissions in the future. For the lakes and rivers, drought is expected to reduce the lake areas (Yu et al., 2004) and decrease regional CH_4 emissions in northeastern China (Region I) and Inner Mongolia.

BGD
12, 7055–7091, 2015

Although short-term expansion in the lakes may occur because of glacial melting over the western plateau of China (Region II and western Region III), water shortages will result in the long-term disappearance of the lakes (Shen et al., 2003a). Fortunately, precipitation is expected to increase, especially in northern China (Region I, Region III and the inland wetlands in Region IV) and on the Qinghai Tibetan Plateau (Region IV) (Ding and Ren, 2007), which may offset the negative impact on CH_4 emissions from the inland wetlands and lakes by the imminent drought conditions. For the coastal wetlands, rising sea levels will reduce the area of coastal wetlands by inundation. Consider the Jiangsu Province in eastern China (Region IV) as an example, where 396, 617 and 1390 km^2 is expected to be lost in the next 30, 50 and 100 years, respectively (Li et al., 2006). Moreover, rising sea levels will increase the invasion of salt water to estuarine wetlands (Shen et al., 2003b; Hu et al., 2003; Huang and Xie, 2000), which will reduce CH_4 fluxes due to the higher salinity.

5 Conclusions

Climate warming increased CH_4 fluxes at a rate of 0.52 $g\,m^{-2}$ per decade from 1950 to 2010. However, during the same period, an estimated 2.35 Tg (1.91–2.81 Tg) of CH_4 reduction in Chinese wetlands occurred, which was mainly due to extensive wetland loss, i.e., from 35.6 to 18.6 million ha. On a national scale, northeastern China experienced a large temperature increase, which resulted in the highest rate of increase in CH_4 fluxes, i.e., 0.67 $g\,m^{-2}$ per decade. However, serious wetland loss made northeastern China become the greatest source of CH_4 decrease, accounting for 70 % of the total CH_4 reduction. The Qinghai Tibetan Plateau had the lowest CH_4 reduction, which was approximately 8 % of the reduction in northeastern China. Among the reduction, the inland wetlands, lakes/rivers and the coastal wetlands accounted for 81, 11 and 8 %, respectively.

BGD
12, 7055–7091, 2015
CH_4 from Chinese natural wetlands
T. Li et al.

The Supplement related to this article is available online at doi:10.5194/bgd-12-7055-2015-supplement.

Author contributions. T. Li, W. Zhang, T. Vesala and M. Raivonen designed the research; Q. Zhang and G. Wang performed the CH_4 modeling; Y. Lu performed the TEM modeling; Z. N. performed the wetland area analysis.

Acknowledgements. This work was supported by the National Natural Science Foundation of China (Grant No. 31000234, 41321064 and 41175132), the Chinese Academy of Sciences (CAS) strategic pilot technology special funds (Grant No. XDA05020204), the Academy of Finland Center of Excellence (Grants No. 1118615 and 272041), ICOS 271878, ICOS-Finland 281255, ICOS-ERIC 281250, Academy Professor projects (1284701 and 1282842) and the Nordic Centre of Excellence DEFROST. We are grateful to Yao Huang in the Institute of Botany, Chinese Academy of Science to provide the valuable recommendations and opinions to this paper. We would also like to thank the Pan-Eurasian Experiment (PEEX)

References

Aerts, R. and Ludwig, F.: Water-table changes and nutritional status affect trace gas emissions from laboratory columns of peatland soils, Soil Biol. Biochem., 29, 1691–1698, 1997.

An, S. Q., Li, H. B., Guan, B. H., Zhou, C. F., Wang, Z. S., Deng, Z. F., Zhi, Y. B., Liu, Y. L., Xu, C., Fang, S. B., Jiang, J. H., and Li, H. L.: China's natural wetlands: past problems, current status, and future challenges, Ambio, 36, 335–342, 2007.

Antonov, J. I., Seidov, D., Boyer, T. P., Locarnini, R. A., Mishonov, A. V., Garcia, H. E., Baranova, O. K., Zweng, M. M., and Johnson, D. R.: World Ocean Atlas 2009 Vol. 2, Salinity, in: NOAA Atlas NESDIS 69, edited by: Levitus, S., US Government Printing Office, Washington, D.C., 1–184, 2010.

Ballantyne, D. M., Hribljan, J. A., Pypker, T. G., and Chimner, R. A.: Long-term water table manipulations alter peatland gaseous carbon fluxes in Northern Michigan, Wetl. Ecol. Manag., 22, 35–47, 2014.

Beven, K. J. and Kirkby, M. J.: A physically based, variable contributing area model of basin hydrology, Hydrolog. Sci. Bull., 24, 43–69, 1979.

Belward, A. S., Estes, J. E., and Kline, K. D.: The IGBP-DIS global 1-km land-cover data set DISCover: a project overview, Photogramm. Eng. Rem. S., 65, 1013–1020, 1999.
Bohn, T. J., Lettenmaier, D. P., Sathulur, K., Bowling, L. C., Podest, E., McDonald, K. C., and Friborg, T.: Methane emissions from western Siberian wetlands: heterogeneity and sensitivity to climate change, Environ. Res. Lett., 2, 045015, doi:10.1088/1748-9326/2/4/045015, 2007.
Boon, P. I., Mitchell, A., and Lee, K.: Effects of wetting and drying on methane emissions from ephemeral floodplain wetlands in southeastern Australia, Hydrobiologia, 357, 73–87, 1997.
Cai, Z. C.: Greenhouse gas budget for terrestrial ecosystems in China, Sci China Ser. D, 55, 173–182, 2012. (FOUND!)
Calhoun, A. and King, G. M.: Regulation of rootassociated methanotrophy by oxygen availability in the rhizosphere of two aquatic macrophytes, Appl. Environ. Microb., 63, 3051–3058, 1997.
Calhoun, A. and King, G. M.: Characterization of root-associated methanotrophs from three freshwater macrophytes: Pontederia cordata, Sparganium eurycarpum, and Sagittaria latifolia, Appl. Environ. Microb., 64, 1099–1105, 1998.
Cao, M. K., Gregson, K., and Marshall, S.: Global methane emission from wetlands and its sensitivity to climate change, Atmos. Environ., 32, 3293–3299, 1998.
Chanton, J. P., Martens, C. S., and Kelley, C. A.: Gas transport from methane-saturated, tidal freshwater and wetland sediments, Limnol. Oceanogr., 34, 807–819, 1989.
Chen, H., Zhu, Q., Peng, C. H., Wu, N., Wang, Y. F., Fang, X. Q., Jiang, H., Xiang, W. H., Chang, X., Deng, X. W., and Yu, G. R.: Methane emissions from rice paddies natural wetlands, lakes in China: synthesis new estimate, Glob. Change Biol., 19, 19–32, 2013.
Christensen, T. and Cox, P.: Response of methane emission from arctic tundra to climate change: results from a model simulation, Geophys. Res. Lett., 31, L04501, doi:10.1029/2003GL018680, 1995.
Christensen, T. R., Ekberg, A., Ström, L., Mastepanov, M., Panikov, N., Öquist, M., Svensson, B. H., Nykänen, H., Martikainen, P. J., and Oskarsson, H.: Factors controlling large scale variations in methane emissions from wetlands, Geophys. Res. Lett., 30, 1414, doi:10.1029/2002GL016848, 2003.
Cicerone, R. J. and Shetter, J. D.: Sources of atmospheric methane: measurements in rice paddies and a discussion, J. Geophys. Res., 86, 7203–7209, 1981.
Collins, W. J., Bellouin, N., Doutriaux-Boucher, M., Gedney, N., Halloran, P., Hinton, T., Hughes, J., Jones, C. D., Joshi, M., Liddicoat, S., Martin, G., O'Connor, F., Rae, J., Senior, C., Sitch, S., Totterdell, I., Wiltshire, A., and Woodward, S.: Development and evaluation of an

Earth-System model – HadGEM2, Geosci. Model Dev., 4, 1051–1075, doi:10.5194/gmd-4-1051-2011, 2011.
Cramer, W., Kicklighter, D. W., Bondeau, A., Moore III, B., Churkina, G., Nemry, B., Ruimy, A., Schloss, A. L., and The Participants of the Potsdam NPP Model Intercomparison: comparing global models of terrestrial net primary productivity (NPP): overview and key results, Glob. Change Biol., 5, 1–15, 1999.
Denman, K. L., Brasseur, G., Chidthaisong, A., Ciais, P., Cox, P. M., Dickinson, R. E., Hauglustaine, D., Heinze, C., Holland, E., Jacob, D., Lohmann, U., Ramachandran, S., da Silva Dias, P. L., Wofsy, S. C., and Zhang, X.: Couplings between changes in the climate system and biogeochemistry, in: Climate Change 2007: The Physical Science Basis. Contribution of Working Group I to the Fourth Assessment Report of the Intergovernmanetal Panel on Climate Change, edited by: Solomon, S., Qin, D., Manning, M., Chen, Z., Marquis, M., Averyt, K. B., Tignor, M., and Miller, H. L., Cambridge University Press, Cambridge, 539–544, 2007.
Ding, W. X, Cai, Z., and Wang, D.: Preliminary budget of methane emissions from natural wetlands in China, Atmos. Environ., 38, 751–759, 2004.
Ding, W. X., Cai, Z., and Tsuruta, H.: Factors affecting seasonal variation of methane concentration in water in a freshwater marsh vegetated with *Carex lasiocarpa*, Biol. Fert. Soils, 41, 1–8, 2005.
Ding, W. X., Cai, Z. C., Tsuruta, H., and Li, X. P.: Effect of standing water depth on methane emissions from freshwater marshes in northeast China, Atmos. Environ., 36, 5149–5157, 2002.
Ding, W. X. and Cai, Z. C.: Methane emission from natural wetlands in China: summary of years 1995–2004 studies, Pedosphere, 17, 475–486, 2007.
Ding, Y. H. and Ren, G. Y.: Climate change in China and its future trend, in: National Assessment Report of Climate Change, edited by: Editing Committee of National Assessment Report of Climate Change, Science Press, China, 130–161, 2007. (in Chinese with English abstract)
Dise, N. B., Gorham, E., and Verry, E. S.: Environmental factors controlling methane emissions from peatlands in Northern Minnesota, J. Geophys. Res.-Atmos., 98, 10583–10584, doi:10.1029/93JD00160, 1993. (FOUND!)

BGD
12, 7055–7091, 2015

Du, X. and Chen, W.: Towards a better understanding of modeling feasibility robustness in engineering design, in: 1999 ASME Design Technical Conference, paper No. DAC-8565, Las Vegas, Nevada, September 1999.

Fan, Y. and Miguez-Macho, G.: A simple hydrologic framework for simulating wetlands in climate and earth system models, Clim. Dynam., 37, 253–278, 2011.

Fan, Y. and van den Dool, H.: Climate prediction center global monthly soil moisture data set at 0.5° resolution for 1948 to present, J. Geophys. Res., 109, D10102, doi:10.1029/2003JD004345, 2004.

FAO/IIASA/ISRIC/ISS-CAS/JRC: Harmonized World Soil Database, version 1.0, FAO, Rome, Italy and IIASA, Laxenburg, Austria, 2008.

FAO/IIASA/ISRIC/ISSCAS/JRC: Harmonized World Soil Database, version 1.2, FAO and IIASA, Rome, Italy and Laxenburg, Austria, 2012.

Forster, P., Ramaswamy, V., Artaxo, P., Berntsen, T., Betts, R., Fahey, D., Haywood, J., Lean, J., Lowe, D., Myhre, G., Nganga, J., Prinn, R., Raga, G., Schulz, M., and Van Dorland, R.: Changes in atmospheric constituents and in radiative forcing, in: Climate Change 2007: The Physical Science Basis. Contribution of Working Group I to the Fourth Assessment Report of the Intergovernmental Panel on Climate Change, edited by: Solomon, S., Qin, D., Manning, M., Chen, Z., Marquis, M., Averyt, K. B., Tignor, M., and Miller, H. L., Cambridge University Press, Cambridge, 131–243, 2007.

Gill, R. and Jackson, R. B.: Global Distribution of Root Turnover in Terrestrial Ecosystems, Oak Ridge National Laboratory Distributed Active Archive Center, Oak Ridge, Tennessee, USA, doi:10.3334/ORNLDAAC/661, 2003.

Grabs, T., Seibert, J., Bishop, K., and Laudon, H.: Modeling spatial patterns of saturated areas: a comparison of the topographic wetness index and a dynamic distributed model, J. Hydrol., 373, 15–23, 2009.

Haitjema, H. M. and Mitchell-Bruker, S.: Are water tables a subdued replica of the topography?, Ground Water, 43, 781–786, 2005.

Harris, I., Jones, P. D., Osborn, T. J., and Lister, D. H.: Updated high-resolution grids of monthly climatic observations – the CRU TS3.10 Dataset, Int. J. Climatol., 34, 623–642, doi:10.1002/joc.3711, 2014.

Holzapfel-Pschorn, A., Conrad, R., and Seiler, W.: Effects of vegetation on the emission of methane from submerged paddy soil, Plant Soil, 92, 223–233, 1986.

Huang, Y., Sun, W., Zhang, W., Yu, Y. Q., Su, Y. H., and Song, C. C. Marshland conversion to cropland in northeast China from 1950 to 2000 reduced the greenhouse effect, Glob. Change Biol., 16, 680–695, 2010.
Huang, Z. G. and Xie, X. D.: Change of the Sea Level and Its Effect and Countermeasures, Guangdong Science and Technology Press, China, 2000.
Hu, S., Zhu, J. R., Fu, D. J., and Wu, H.: Estuarine circulation and saltwater intrusion II: impacts of river discharge and rise of sea level, J. Ocean University Qingdao, 33, 337–342, 2003. (in Chinese with English abstract)
IPCC: Emission Scenarios: a Special Report of Workgroup III of IPCC, Cambridge University Press, UK, 2000.
IPCC: Climate Change 2007: The Physical Science Basis. Contribution of Working Group I to the Fourth Assessment Report of the Intergovernmental Panel on Climate Change, edited by: Solomon, S., Qin, D., Manning, M., Chen, Z., Marquis, M., Averyt, K. B., Tignor, M., and Miller, H. L., Cambridge University Press, Cambridge, 2007.
IPCC: Climate Change 2013: The Physical Science Basis. Contribution of Working Group I to the Fifth Assessment Report of the Intergovernmental Panel on Climate Change, edited by: Stocker, T. F., Qin, D., Plattner, G. K., Tignor, M., Allen, S. K., Boschung, J., Nauels, A., Xia, Y., Bex, V., and Midgley, P. M., Cambridge University Press, Cambridge, 2013.
Jin, H. J., Wu, J., Cheng, G. D., Tomoko, N., and Sun, G. Y.: Methane emissions from wetlands on the Qinghai-Tibet Plateau, Chinese Sci. Bull., 44, 2282–2286, 1999.
Juutinen, S., Larmola, T., Remus, R., Mirus, E., Merebach, W., Silvola, J., and Augustin, J.: The contribution of *Phragmites australis* litter to methane emission in planted and non-planted fen microcosms, Biol. Fert. Soils, 38, 10–14, 2003.
Khalil, M. A. K., Shearer, M. J., and Rasmussen, R. A.: Methane sources in China: historical and current emissions, Chemosphere, 26, 127–142, 1993.
King, G. M.: Associations of methanotrophs with roots and rhizomes of aquatic vegetation, Appl. Environ. Microb., 60, 3220–3227, 1994.
King, J. Y. and Reeburgh, W. S.: A pulse-labeling experiment to determine the contribution of recent plant photosynthates to net methane emission in arctic wet sedge tundra, Soil Biol. Biochem., 34, 173–180, 2002.
King, J. Y., Reeburgh, W. S., Thieler, K. K., Kling, G. W., Loya, W. M., Johnson, L. C., and Nadelhoffer, K. J.: Pulse-labeling studies of carbon cycling in Arctic tundra ecosystems:

the contribution of phytosynthates to methane emission, Global Biogeochem. Cy., 16, 1062, doi:10.1029/2001GB001456, 2002.

Kleinen, T., Brovkin, V., and Schuldt, R. J.: A dynamic model of wetland extent and peat accumulation: results for the Holocene, Biogeosciences, 9, 235–248, doi:10.5194/bg-9-235-2012, 2012.

Laiho, R.: Decomposition in peatlands: reconciling seemingly contrasting results on the impacts of lowered water levels, Soil Biol. Biochem., 38, 2011–2024, 2006.

Lang, H. Q. and Zu, W. C.: Marshland in Chinese, Shandong Science and Technology Press, China, 1983.

Li, J. L., Wang, Y. H., Zhang, R. S., Qi, D. L., and Zhang, D. F.: Disaster effects of sea level rise – a case of Jiangsu coastal low land, Sci. Geograph. Sinica, 26, 87–93, 2006. (in Chinese with English abstract)

Li, T., Huang, Y., Zhang, W., and Song, C.: $CH4MOD_{wetland}$: a biogeophysical model for simulating CH_4 emissions from natural wetland, Ecol. Model., 221, 666–680, 2010.

Li, T., Huang, Y., Zhang, W., and Yu, Y.-Q.: Methane emissions associated with the conversion of marshland to cropland and climate change on the Sanjiang Plain of northeast China from 1950 to 2100, Biogeosciences, 9, 5199–5215, doi:10.5194/bg-9-5199-2012, 2012.

Lin, E. D., Wu, S. H., and Luo, Y.: Climate change impacts and adaptation, in: The Second National Assessment Report of Climate Change, edited by: Editing Committee of the Second National Assessment Report of Climate Change, Science Press, China, 195–339, 2011 (in Chinese with English abstract).

Liu, J., Tian, H., Liu, M., Zhuang, D., Melillo, J. M., and Zhang, Z.: China's changing landscape during the 1990s: large-land transformations estimated with satellite data, Geophys. Res. Lett., 32, L02405, doi:10.1029/2004GL021649, 2005.

Liu, M. and Tian, H.: China's land cover and land use change from 1700 to 2005: estimations from high-resolution satellite data and historical archives, Global Biogeochem. Cy., 24, GB3003, doi:10.1029/2009GB003687, 2010.

Liu, X. T. and Ma, X. H.: Influence of large scale reclamation on natural environment and regional environmental protection in the Sanjiang Plain, Sci. Geograph. Sinica, 20, 14–19, 2000. (in Chinese with English abstract)

Liu, Z. Q., Liu, H. Y., and Lv, X. G.: Ecological fragility of wetlands in Sanjiang Plain, Chinese J. Appl. Ecol., 12, 241–244, 2001. (in Chinese with English abstract)

Loya, W. M., Johnson, L. C., Kling, G. W., King, J. Y., Reeburgh, W. S., and Nadelhoffer, K. J.: Pulse-labeling studies of carbon cycling in arctic tundra ecosystems: contribution of photosynthesis to soil organic matter, Global Biogeochem. Cy., 16, 1101, doi:10.1029/2001GB001464, 2002.

Loveland, T. R., Brown, J. F., Ohlen, D. O., Zhu, Z., Yang, L., Merchant, J. W., and Reed, B. C.: Development of a global land cover characteristics database and IGBP DISCover from 1 km AVHRR data, Int. J. Remote Sens., 21, 1303–1330, 2000.

Lu, X. and Zhuang, Q.: Modeling methane emissions from the Alaskan Yukon River basin, 1986–2005, by coupling a larg-scale hydrological model and a process-based methane model, J. Geophys. Res., 117, G02010, doi:10.1029/2011JG001843, 2012.

Marthews, T. R., Dadson, S. J., Lehner, B., Abele, S., and Gedney, N.: High-resolution global topographic index values for use in large-scale hydrological modelling, Hydrol. Earth Syst. Sci., 19, 91–104, doi:10.5194/hess-19-91-2015, 2015.

McGuire, A. D., Melillo, J. M., Joyce, L. A., Kicklighter, D. W., Grace, A. L., Moore III, B., and Vorosmarty, C. J.: Interactions between carbon and nitrogen dynamics in estimating net primary productivity for potential vegetation in North America, Global Biogeochem. Cy., 6, 101–124, 1992.

Megonigal, J. P., Whalen, S. C., Tissue, D. T., Bovard, B., Allen, A., Alberts, D., and Schlesinger, W. H.: The use $^{14}CO_2$ to trace carbon metabolism from photosynthesis through methanogenesis in a wetland plant-soil–atmosphere microcosm, Fourth Symposium on Biogeochemistry of Wetlands, New Orleans, Louisiana, USA, 1996.

Melillo, J. M., Mcguire, A. D., Kicklighter, D. W., Moore, B., Vorosmarty, C. J., and Schloss, A. L.: Global climate change and terrestrial net primary production, Nature, 363, 234–240, 1993.

Mitsch, J. W. and Gosselink, J. G.: Wetlands, 4th edn., John Wiley and Sons Inc, Hoboken, NJ, 2007.

Moser, M., Prentice, C., and Frazier, S.: A global overview of wetland loss and degradation, Proceedings to the 6th Meeting of the Conference of Contracting Parties of the Ramsar Convention, Brisbane, Australia, Vol. 10/12B, 21–31, 1996.

Niu, Z. G., Zhang, H. Y., Wang, X. W., Yao, W. B., Zhou, D. M., Zhao, K. Y., Zhao, H., Li, N. N., Huang, H. B., Li, C. C., Yang, J., Liu, C. X., Liu, S., Wang, L., Li, Z., Yang, Z. Z., Qiao, F., Zheng, Y. M., Chen, Y. L., Sheng, Y. W., Gao, X. H., Zhu, W. H., Wang, W. Q., Wang, H., Weng, Y. L., Zhuang, D. F., Liu, J. Y., Luo, Z. C., Cheng, X., Guo, Z. Q., and Gong, P.:

Mapping wetland changes in China between 1978 and 2008, Chinese Sci. Bull., 57, 2813–2823, 2012.
Nisbet, E. G., Dlugokencky, E. J., and Bousquet, P.: Methane on the rise-again, Science, 343, 493–495, 2014.
Nykanen, H., Alm, J., Silvola, J., Tolonen, K., and Martikainen, P. J.: Methane fluxes on boreal peatlands of different fertility and the effect of long-term experimental lowering of the water table on flux rates, Global Biogeochem. Cy., 12, 53–69, 1998.
Potter, C., Klooster, S., Hiatt, S., Fladeland, M., Genovese, V., and Gross, P.: Methane emissions from natural wetlands in the United States: satellite-derived estimation based on ecosystem carbon cycling, Earth Interact., 10, 1–12, 2006.
Revenga, C., Brunner, J., Henninger, N., Kassem, K., and Payne, R.: Pilot Analysis of Global Ecosystems: Freshwater Systems, World Resources Institute, Washington, DC, 2000.
Schimel, J. P.: Plant transport and methane production as controls on methane flux from arctic wet meadow tundra, Biogeochemistry, 28, 183–200, 1995.
Shindell, D. T., Walter, B. P., and Faluvegi, G.: Impacts of climate change on methane emissions from wetlands, Geophys. Res. Lett., 31, L21202, doi:10.1029/2004GL021009, 2004.
Shindell, D. T., Faluvegi, G., Koch, D. M., Schmidt, G. A., Unger, N., and Bauer, S. E.: Improved attribution of climate forcing to emissions, Science, 326, 716–718, 2009.
Shen, H. T., Mao, Z. C., and Zhu, J. R.: Salt Water Intrusion in Changjiang Estuary, China Ocean Press, China, 2003. (in Chinese with English abstract)
Shen, Y. P., Liu, S. Y., Ding, Y. J., and Wang, S. D.: Glacier mass balance change in Tailanhe river watersheds on the south slope of the Tianshan Mountains and its impact on water resources, J. Glaciol. Geocryol., 25, 124–129, 2003 (in Chinese with English abstract).
Strack, M. and Waddington, J. M.: Response of peatland carbon dioxide and methane fluxes to a water table drawdown experiment, Global Biogeochem. Cy., 21, GB1007, doi:10.1029/2006GB002715, 2007.
Tian, H., Xu, X., Lu, C., Liu, M. L., Ren, W., Chen, G. S., Melillo, J., and Liu, J. Y.: Net exchanges of CO_2, CH_4, and N_2O between China's terrestrial ecosystems and the atmosphere and their contributions to global climate warming, J. Geophys. Res., 116, G02011, doi:10.1029/2010JG001393, 2011.
Turetsky, M. R., Treat, C. C., Waldrop, M. P., Waddington, J. M., Harden, J. W., and McGuire, A. D.: Short-term response of methane fluxes and methanogen activity to water ta-

ble and soil warming manipulations in an Alaskan peatland, J. Geophys. Res., 113, G00A10, doi:10.1029/2007JG000496, 2008.
USGS: US Geological Survey: HYDRO1k Elevation derivative database, US Geological Survey Earth Resources Observation and Science (EROS) Center, Sioux Falls, South Dakota, 2000.
Wang, M. X., Dai, A. G., Huang, J., Ren, L. X., and Shen, R. X.: Sources of methane in China: rice fields, agricultural waste treatment, cattle, coal mines, and other minor sources, Scientia Atmospherica Sinica, 17, 52–64, 1993. (in Chinese with English abstract)
Wang, X. K., Lu, F., and Yang, L.: Methane emissions from China's natural wetlands: measurements, temporal variations and influencing factors, in: Recarbonization of the Biosphere, edited by: Lal, R., Lorenz, K., Hüttl, R. F., Schneider, B. U., and von Braun, J., Springer, the Netherlands, 99–125, 2012.
Waddington, J. M. and Roulet, N. T.: Atmosphere-wetland carbon exchanges: scale dependency of CO_2 and CH_4 exchange on the developmental topography of a peatland, Global Biogeochem. Cy., 10, 233–245, 1996.
Whalen, S. C.: Biogeochemistry of methane exchange between natural wetlands and the atmosphere, Environ. Eng. Sci., 22, 73–94, 2005.
Wieder, R. K., Yavitt, J. B.: Peatlands and global climate change: insights from comparative studies of sites situated along a latitudinal gradient, Wetlands, 14, 229–238, 1994.
Xu, X. and Tian, H.: Methane exchange between marshland and the atmosphere over China during 1949–2008, Global Biogeochem. Cy., 26, GB2006, doi:10.1029/2010GB003946, 2012.
Yang, W. Y., Song, C. C., and Zhang, J. B.: Dynamics of methane emissions from a freshwater marsh of northeast China, Sci. Total Environ., 371, 286–292, 2006.
Yrjala, K., Tuomivirta, T., Juottonen, H., Putkinen, A., Lappi, K., and Tuittila, E. S.: CH_4 production and oxidation processes in a boreal fen ecosystem after long-term water table drawdown, Glob. Change Biol., 17, 1311–1320, 2011.
Yu, G., Lai, L. B., and Xu, B.: Preliminary Study on the responses of lake water from the western China to climate change in the future: Monte carlo analysis applied in GCM simulations and lake water changes, J. Lake Sci., 16, 193–202, 2004. (in Chinese with English abstract)
Yu, K. W., Wang, Z. P., Vermoesen, A., Patrick Jr, W. H., and Cleemput, O. V.: Nitrous oxide and methane emissions from different soil suspensions: effect of soil redox status, Biol. Fert. Soils, 34, 25–30, 2001.

BGD
12, 7055–7091, 2015

CH_4 from Chinese natural wetlands

T. Li et al.

Zhang, X., Jiang, H., Lu, X., Cheng, M., Zhang, X., Li, X., and Zhang, L.: Estimate of methane release from temperate natural wetlands using ENVISAT/SCIAMACHY data in China, Atmos. Environ., 69, 191–197, 2013.

Zhuang, Q., Melillo, J., Kicklighter, D., Prinn, R. G., McGuire, A. D., Steudler, P. A., Felzer, B. S., and Hu, S.: Methane fluxes between terrestrial ecosystems and the atmosphere at northern high latitudes during the past century: a retrospective analysis with a process-based biogeochemistry model, Global Biogeochem. Cy., 18, GB3010, doi:10.1029/2004GB002239, 2004.

Zhuang, Q., Mellillo, J., Sarofim, M., Kicklighter, D. W., McGuire, A. D., Felzer, B. S., Sokolov, A., Prinn, R. G., Steudler, P. A., and Hu, S: CO_2 and CH_4 exchanges between land ecosystems and the atmosphere in northern high latitudes over the 21st century, Geophys. Res. Lett., 33, L17403, doi:10.1029/2006GL026972, 2006.

Zhuang, Q., Melillo, J., Mcguire, A., Kicklighter, D., Prinn, R. G., Steudler, P. A., Felzer, B. S., and Hu, S.: Net emissions of CH_4 and CO_2 in Alaska: implications for the region's greenhouse gas budget, Ecol. Appl., 17, 203–212, 2007.

Zhuang, Q., Chen, M., Xu, K., Tang, J., Saikawa, E., Lu, Y., Melillo, J. M., Prinn, R. G., and McGuire, A. D.: Response of global soil consumption of atmospheric methane to changes in atmospheric climate and Nitrogen deposition, Global Biogeochem. Cy., 27, 650–663, 2013.

Zhu, X. D., Zhuang, Q. L., Xiang, G., Sokolov, A., and Schlosser, C. A.: Pan-Arctic land-atmospheric fluxes of methane and Carbon dioxide in response to climate change over the 21st century, Environ. Res. Lett., 8, 045003, doi:10.1088/1748-9326/8/4/045003, 2013.

Table 1. Regional CH_4 emissions and the wetland area.

		Region CH_4 emissions[a] (Tg)						Area[b] (M ha)					
		I	II	III	IV	V	China	I	II	III	IV	V	China
Inland Wetland	1950	2.80	0.31	0.25	0.06	0.11	3.53	12.26	4.78	2.66	0.30	0.27	20.27
	1980	2.06	0.27	0.22	0.06	0.10	2.71	9.71	4.61	2.57	0.29	0.26	17.44
	1990	1.90	0.23	0.14	0.09	0.08	2.44	7.73	3.42	1.77	0.44	0.18	13.54
	2000	1.13	0.23	0.13	0.05	0.07	1.61	5.40	3.43	1.41	0.23	0.15	10.62
	2010	1.16	0.22	0.12	0.05	0.06	1.61	5.09	3.20	1.36	0.20	0.13	9.98
	Decrease[c]	−58.6 %	−29.0 %	−50.40 %	−16.7 %	−45.5 %	−54.4 %	−58.2 %	−33.3 %	−48.1 %	−33.3 %	−66.7 %	−50.8 %
Coastal Wetland	1950	lt	nw	nw	0.09	0.18	0.27	lt	nw	nw	1.52	1.02	2.54
	1980	lt	nw	nw	0.08	0.09	0.17	lt	nw	nw	0.78	0.53	1.31
	1990	lt	nw	nw	0.05	0.07	0.12	lt	nw	nw	0.75	0.4	1.15
	2000	lt	nw	nw	0.05	0.06	0.11	lt	nw	nw	0.54	0.37	0.91
	2010	lt	nw	nw	0.06	0.04	0.10	lt	nw	nw	0.53	0.27	0.80
	Decrease[c]	lt	nw	nw	−33.3 %	−77.8 %	−62.9 %	lt	nw	nw	−65.1 %	−73.5 %	−68.5 %
Lakes and Rivers	1950	0.08	0.29	0.08	0.22	0.04	0.70	1.38	5.19	1.49	4.05	0.68	12.79
	1980	0.07	0.26	0.07	0.20	0.03	0.62	1.20	4.62	1.27	3.55	0.56	11.21
	1990	0.05	0.22	0.04	0.13	0.03	0.47	0.91	3.83	0.78	2.32	0.51	8.35
	2000	0.04	0.22	0.04	0.11	0.03	0.45	0.76	3.87	0.77	1.93	0.61	7.94
	2010	0.04	0.25	0.04	0.07	0.04	0.44	0.79	4.32	0.78	1.31	0.65	7.85
	Decrease[c]	−50.0 %	−13.8 %	−50.0 %	−68.2 %	0.0 %	−37.1 %	−42.8 %	−16.8 %	−47.7 %	−67.7 %	−4.4 %	−38.6 %
Total Wetland	1950	2.88	0.60	0.33	0.37	0.33	4.50	13.64	9.97	4.15	5.87	1.97	35.60
	1980	2.13	0.53	0.29	0.34	0.22	3.50	10.91	9.23	3.84	4.62	1.35	29.96
	1990	1.95	0.45	0.18	0.27	0.18	3.03	8.64	7.25	2.55	3.51	1.09	23.04
	2000	1.17	0.45	0.17	0.21	0.16	2.17	6.16	7.3	2.18	2.7	1.13	19.47
	2010	1.20	0.47	0.16	0.18	0.14	2.15	5.88	7.52	2.14	2.04	1.05	18.63
	Decrease[c]	−58.3 %	−23.3 %	−51.5 %	−51.4 %	−57.6 %	−52.2 %	−56.9 %	−24.6 %	−48.4 %	−65.3 %	−46.7 %	−47.7 %

[a] The average CH_4 fluxes of three consecutive years (including 1950–1952, 1979–1981, 1989–1991, 1999–2001 and 2008–2010) were used to calculated regional CH_4 emissions. For example, regional CH_4 emissions in 1980 were the production of the area of 1980 and the average CH_4 fluxes from 1979 to 1981.
[b] Data of 1980, 1990, 2000 and 2010 were from the remote sensing data (Niu et al., 2012). The area of 1978 and 2008 were regarded as the area of 1980 and 2010, respectively.
[c] Decrease means the reduce fraction in 2010 compared with 1950.
lt, less than 0.0001; nw, no wetland.

Table 2. Estimation of CH_4 emissions from natural wetland in China.

Region	This study			Other studies			References
	CH_4 (Tg)	Period	Area (Mha)	CH_4 (Tg)	period	Area (Mha)	
China[a]	3.0	1990	23.0	2.2	1988–2000	Nm	Wang et al. (1993)
China[a]	3.0	1990	23.0	1.7	1988	Nm	Khalil et al. (1993)
China[a]	3.0	1990	23.0	2.0	1996	18.7	Jin et al. (1999)
China[a]	3.0	1990	23.0	10.5	1990s	38.0	Wang et al. (2012)
China[a]	3.0	1990	23.0	6.65	1990	35.5	Cai (2012)
China[a]	2.2	2000	19.5	5.71	2000	30.5	Cai (2012)
China[a]	2.2	2000	19.5	3.15	2000	Nm	Chen et al. (2013)
China[a]	2.2	2000	19.5	4.76	2003–2009	9.0	Zhang et al. (2013)
China[b]	3.5	1950	20.3	3.2	1950	17.9	Xu and Tian (2012)
China[b]	2.7	1980	17.4	2.3	1980	13.0	Xu and Tian (2012)
China[b]	2.4	1990	13.5	2.0	1990	11.0	Xu and Tian (2012)
China[b]	1.6	2000	10.6	1.9	2000	9.4	Xu and Tian (2012)
China[b]	1.6	2010	10.0	1.9	2008	9.4	Xu and Tian (2012)
China[b]	1.6	2000	10.6	1.9	1995–2004	9.4	Tian et al. (2011)
China[b]	1.6	2000	10.6	1.8	1995–2004	9.4	Ding et al. (2007)
NYC[b]	2.8	1950	12.3	2.2	1950	10.1	Xu and Tian (2012)
NYC[b]	1.2	2010	5.1	1.2	2008	4.7	Xu and Tian (2012)
NYC[b]	1.1	2000	5.4	1.2	2001–2002	2.8	Ding et al. (2004)
NYC[b]	1.1	2000	5.4	0.9	2000	Nm	Chen et al. (2013)
QHT[b]	0.3	1950	4.8	0.07	1950	0.8	Xu and Tian (2012)
QHT[b]	0.2	2008	3.2	0.06	2008	0.6	Xu and Tian (2012)
QHT[a]	0.45	1990	7.3	0.8	1996	3.5	Jin et al. (1999)
QHT[b]	0.23	2000	3.4	0.56	2001–2002	4.8	Ding et al. (2004)
QHT[b]	0.23	2000	3.4	1.25	2000	Nm	Chen et al. (2013)

[a] Natural wetland.
[b] Natural wetland exclude coastal wetland, lakes and rivers.
Nm, not mentioned in the literature.
NYC, Northeast China.
QTH, Qinghai Tibetan Plateau.

BGD
12, 7055–7091, 2015

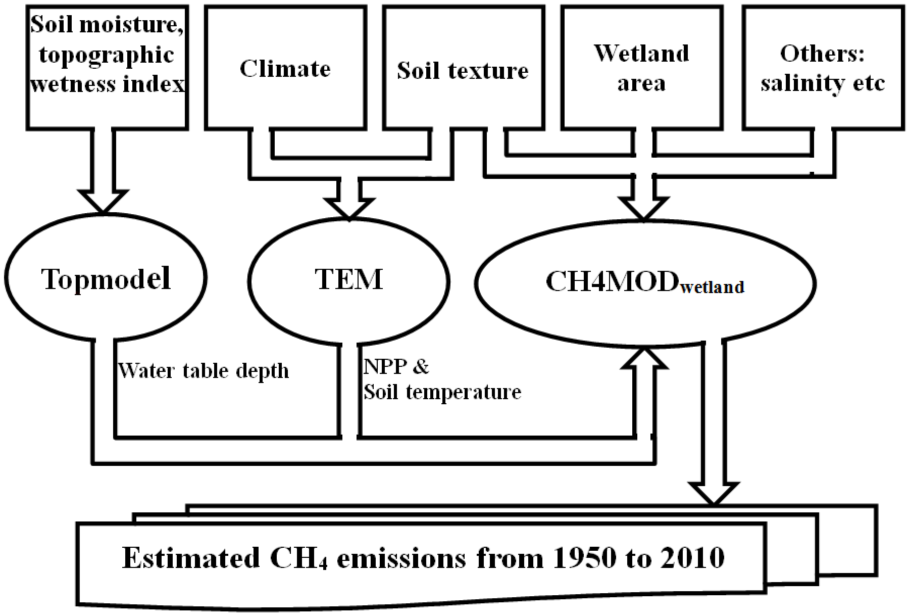

Figure 1. Framework of simulating CH_4 emissions from natural wetlands between 1950 and 2010. $CH4MOD_{wetland}$ is a biogeophysical model to simulate CH_4 fluxes from natural wetlands. TEM is a process-based biogeochemistry model that couples carbon, nitrogen, water, and heat processes in terrestrial ecosystems to simulate ecosystem carbon and nitrogen dynamics. TOPMODEL is a conceptual rainfall–runoff model that is designed to work at the scale of large watersheds using the statistics of topography.

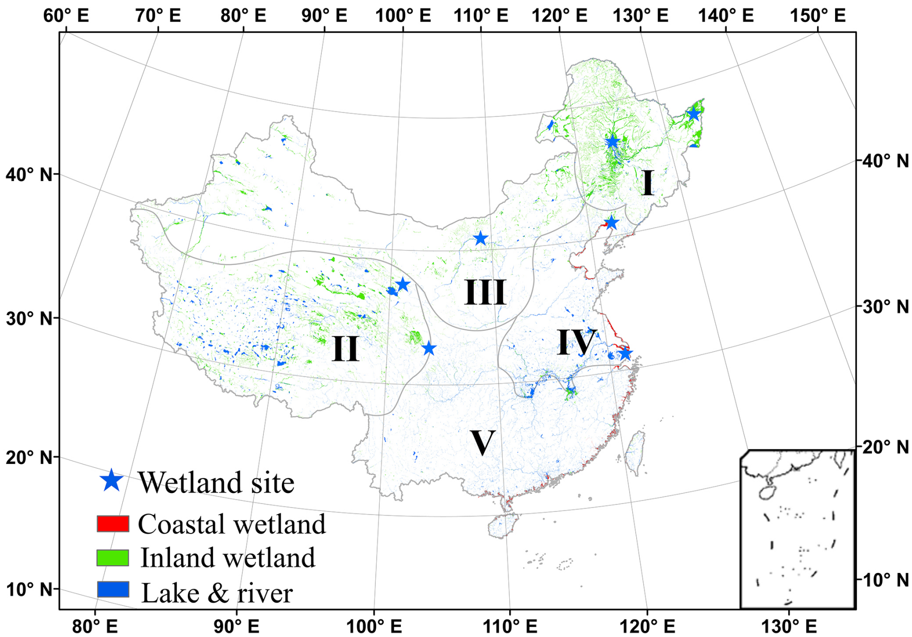

Figure 2. Wetland regions across China. The blue stars are the locations of the wetland sites.

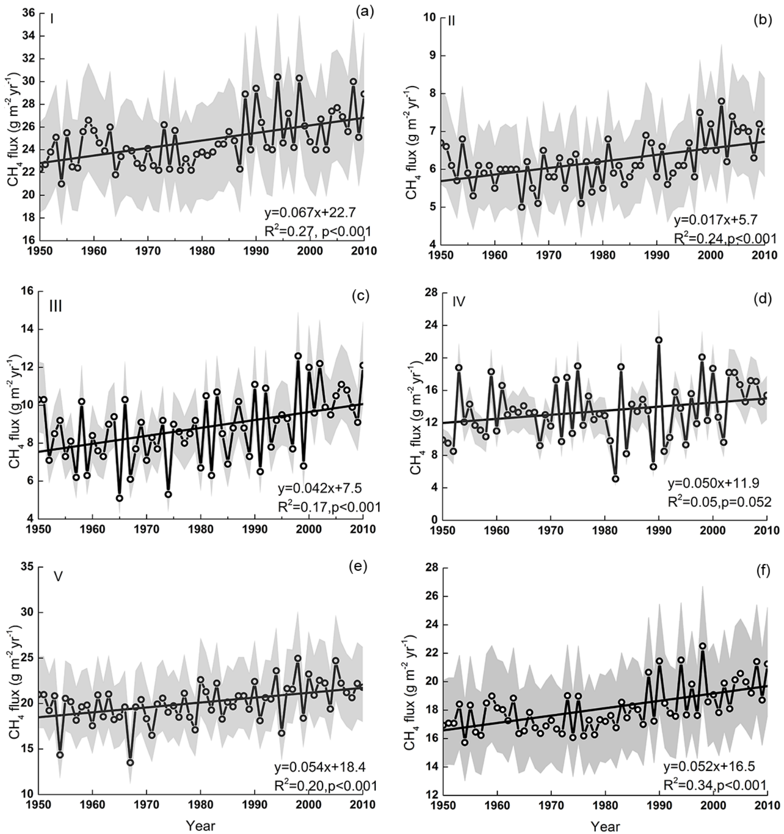

Figure 3. Methane fluxes from inland and coastal wetlands between 1950 and 2010 in: **(a)** Region I; **(b)** Region II; **(c)** Region III; **(d)** Region IV; **(e)** Region V. **(f)** China.

BGD

12, 7055–7091, 2015

Title Page
Abstract | Introduction
Conclusions | References
Tables | Figures
◀| |▶
◀ ▶
Back | Close
Full Screen / Esc
Printer-friendly Version
Interactive Discussion

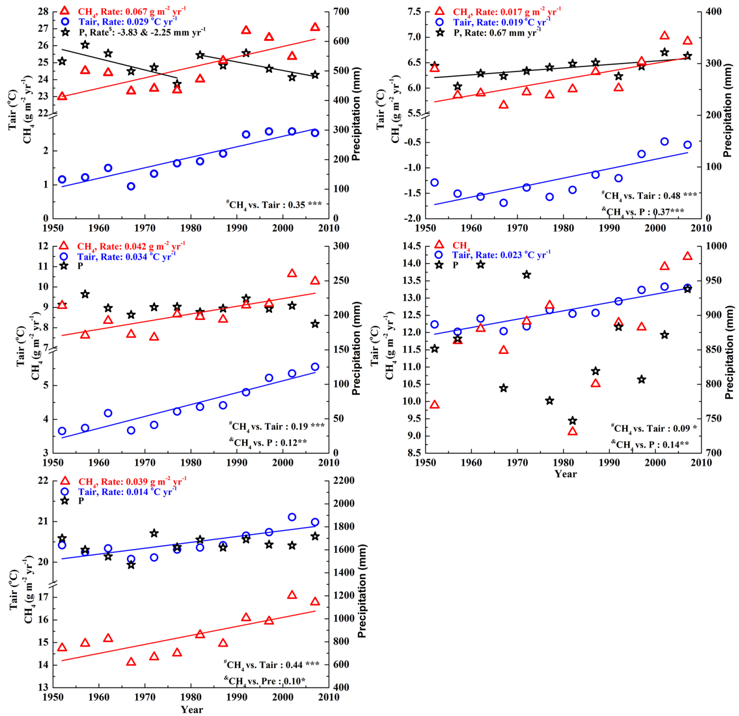

Figure 4. Impact of the climate factors on CH_4 fluxes from 1950 to 2010 in: **(a)** Region I; **(b)** Region II; **(c)** Region III; **(d)** Region IV; and **(e)** Region V. The red triangles, blue circles and the black stars are 5 year average CH_4 fluxes (the same data as in Fig. 3), air temperature and precipitation, respectively. The slope represents the significant linear rate ($p < 0.05$). CH_4 vs. Tair: the correlation coefficient between the annual mean CH_4 fluxes and air temperature at a significantly. CH_4 vs. P: the correlation coefficient between the annual mean CH_4 fluxes and the precipitation. Only correlations with statistical significance are shown ($p < 0.05$).

BGD

12, 7055–7091, 2015

CH_4 from Chinese natural wetlands

T. Li et al.

Title Page
Abstract | Introduction
Conclusions | References
Tables | Figures
◂◂ | ▸▸
◂ | ▸
Back | Close
Full Screen / Esc
Printer-friendly Version
Interactive Discussion